International Journal of Advanced Research in Physical Science (IJARPS)
Volume 3, Issue 4, 2016, PP 24-34
ISSN 2349-7874 (Print) & ISSN 2349-7882 (Online)
www.arcjournals.org

Piezoelectric and Dielectric Characterization of BNBT6: 4Eu Ceramics

[1]D.Gangadharudu, [2]B.Venkateswara Rao, [3]Y.N.Ch.Ravi Babu, [4]B.Jhansi Lakshmi

[1]S.R.V.B.S.J.B.M.R.College, Peddapuram, East Godavari Dt., A.P., India
[2]S.S. & N. College, Narasaraopeta, Guntur Dt., A.P., India
[3]The Hindu College, Machilipatnam, Krishna Dt., A.P., India
[4]Govt. Degree College, Avanigadda, Krishna Dt., A.P., India
ynchravibabu@gmail.com

Abstract: *We have prepared lead-free polycrystalline ($Bi_{0.94-x}Eu_xNa_{0.94})_{0.5}Ba_{0.06}TiO_3$ (x = 0.04, designated as BNBT6:4Eu) ceramics by mixed oxide technique. The authors have followed unique approach for synthesizing the sample (which has not been reported by previous researchers) to obtain optimal conditions (such as stay time, maximum applied pressure, sintering temperature and holding time). We have successfully prepared a highly dens BNBT6:4Eu ceramic. The formation of single-phase material was confirmed by X-ray studies. Uniformly distributed rectangular grains of average grain size equal to 1.137 μm have been obtained. It is known the rhombohedral symmetry of BNT ceramics at room temperature is characterized by a single peak of (202) between 45-48^0 and a (003)/(021) peak splitting between 39-42^0[1, 2]. The XRD result has indicated a distinct (002)/(200) peak splitting between 45-48^0 corresponding to a tetragonal symmetry[1, 2]. Therefore, the rhombohedral and tetragonal phases coexist in the BNBT6-4Eu sample, which is consistent with its nature as a composition near the morphotropic phase boundary (MPB)[3, 4]. Energy dispersive X-ray analysis spectrum confirmed the elements present in the prepared sample are only Na, Bi, Ba, Ti, O and Eu. The BNBT6-4Eu sample has very good piezoelectric properties with k_p = 25 %, d_{33} = 158 pC/N. From the piezoelectric d coefficient in thickness mode, we obtained the change in the thickness of the ceramic sample, Δt = 15.8 nm for an applied voltage of 100V. The obtained values of d_{33}, k_p, and Δt imply the BNBT6-4Eu sample could be useful in actuator devices. The dielectric constant and dielectric loss as a function of temperature (35^{0}C – 500^{0}C) and frequency (100Hz – 1MHz) has been studied. Diffuse phase transition (DPT) behavior with a diffuseness constant (γ) = 1.88 at a frequency of 1 kHz was obtained for the BNBT6:4Eu sample which indicates a more diffuseness behavior. Impedance (real Z') plots provide an indication of increasing conduction with temperature and frequency i.e., behavior similar to a semiconductor exhibiting negative temperature coefficient of resistance. CIS analysis suggests the presence of temperature-dependent relaxation process in the material. Cole – Cole plots confirm charge conduction takes place through the grains. The activation energies have been calculated from impedance E_τ = 0.57 eV studies, which suggests that the conduction is ionic in nature due to the involvement of relaxation process by mobile charge carriers hopping through oxygen vacancies at higher temperatures.*

Keywords: *Synthesis, X-ray diffraction, BNBT6, lead – free, diffuse phase transition*

1. INTRODUCTION

Piezoelectric materials used as sensors, actuators, filters, resonators, and different microelectronic devices have been produced mainly from polycrystalline ferroelectric materials having after poling, a remarkable remnant polarization below a temperature called Curie point (T_C). But, theses materials are mainly lead-based piezoelectric ceramics, such as PZT, PMN and PZLT [1–3].

However there are concerns regarding the preparation, application and disposal of such lead-based devices because of the volatility and toxicity of lead oxide [2–4]. As a result, there is a great deal of continuous research towards producing environmental friendly and lead-free piezoelectric materials in the past few decades. Bismuth sodium titanate ($Bi_{0.5}Na_{0.5}TiO_3$ – BNT) discovered in 1960 by Smolenskii *et al.*,[5] was considered to be a promising replacement to the lead-based piezoelectric ceramics. Because BNT has high Curie temperature (320^{0}C) and a relatively large remnant polarization (38μC/cm^2) at room temperature. But, because of a relatively high coercive field (73kV/cm) and high conductivity [6], it is difficult to pole pure BNT.

Tu, *et al*., and Jan Suchanicz [7–9] have studied various properties of pure BNT ceramics. To overcome the poling problem and improve the electric properties, researchers have developed and studied BNT based solid solutions and BNT ceramics with additives, such as Eu_2O_3 doped BNT [10], Ce^{3+} and Sm^{3+} doped BNT [11], Dy–doped BNT [12], Nd and Nb doped BNT [13], and BNT–BT solid solutions [14].

The $(Bi_{0.5}Na_{0.5})_{1-x}$-Ba_xTiO_3 system has attracted considerable attention, because of its high piezoelectric properties, reported to be due to the presence of a rhombohedral–tetragonal morphotropic phase boundary (MPB) near x = 0.06[14]. To further enhance the piezoelectric properties of the $(Bi_{0.5}Na_{0.5})_{1-x}$-Ba_xTiO_3 system at x = 0.06, different additives were investigated, such as Dy_2O_3 [2], $CeO_2 + La_2O_3$ [6], La_2O_3 [4], Nb_2O_5, Co_2O_3 and La_2O_3 [15], CeO_2 [16] and Y_2O_3 [17]. However, much of the focus of these studies has been on the effect of additives on dielectric and piezoelectric properties. There is very little report on effect of Eu_2O_3 substitution on $(Bi_{0.5}Na_{0.5})_{1-x}$-Ba_xTiO_3 (at x = 0.06). In the present study, synthesis, piezoelectric and dielectric characterization of Eu_2O_3 substituted $\mathbf{(Bi_{0.94}Na_{0.94})_{0.5}Ba_{0.06}TiO_3}$ has been investigated for device applications.

2. SYNTHESIS AND CERAMIC PROCESSING

Eu_2O_3 substituted $(Bi_{0.94}Na_{0.94})_{0.5}Ba_{0.06}TiO_3$ (x = 0, 0.04 and 0.08) ferroelectric ceramics were prepared by the conventional solid state reaction method. The starting materials are AR grade and high purity (99%+) oxides and carbonate powders of $BaCO_3$, Bi_2O_3, Na_2CO_3, Eu_2O_3, and TiO_2. The powders were weighed according to their respective stoichiometric ratios given by the following solid state reaction

$Bi_2O_3 + Na_2CO_3 + Eu_2O_3 + BaCO_3 + TiO_2 \rightarrow (Bi_{0.94-x}Eu_xNa_{0.94})_{0.5}Ba_{0.06}TiO_3 + CO_2\uparrow$ (x = 0.04 designated as BNBT6: 4Eu)

3wt.% excess amounts of Bi_2O_3 and Na_2CO_3 were added to compensate for the weight loss during high temperature treatment. The powder mixture has been thoroughly ground (dry and wet) using agate mortar and pestle until it became a dry fine powder [18]. The powder was placed in a closed platinum crucible and calcined at 800^0C for 2h. This was done twice to achieve a homogeneous, single – phase material. X-ray powder diffraction analysis was taken at room temperature with a Philips Diffractometer using CuKα radiation (λ = 1.54059Å) for a wide range of Bragg angle, 2θ ($0 < 2\theta < 90^0$). The XRD peaks were indexed by using a standard computer program 'POWD' (Interpretation and Indexing Program, Version 2.2, by E. Wu, School of Physical Sciences, Flinders University of South Australia, Bedford Park, S. A. 5042, Australia). After checking the phase purity, enough amount of Polyvinyl Alcohol (PVA) was added as binder to the pre-sintered powder and granulated well. Then ceramic discs of 2mm thickness and 11.50mm diameter were pressed using uni-axial hydraulic press. The green pellets sintered for 4h at 1135^0C exhibited optimum density.

For electrical measurements, both surfaces of the pellets were screen plated with silver paste as electrodes and fired at 600^0C for 20 minutes. Then the pellets were poled under a DC field of 4.5 kV/mm in a silcon oil bath at 80^0C for 20 minutes. Capacitance, dissipation and impedance measurements were carried out over a wide frequency range (100–1MHz) and temperature range (30–500^0C) by using computer interfaced Phase Sensitive Multimeter (PSM1700 PsimetriQ). For SEM and EDS studies, the pellets were thermally etched [19] at a temperature which is 15^0C less than the sintering temperature of the sample. The average grain size was measured using line intercept method on SEM micrographs obtained using Carl Zeiss SEM (Model-EVO M A 15) enabled with EDS (Oxford instruments, Inca Penta FET x 3)

3. RESULTS AND DISCUSSION

3.1. Structure

The Goldschmidt tolerance factor t is obtained by using the expression [3]:

$$t = \frac{R_A + R_O}{\sqrt{2}(R_B + R_O)}$$

where R_A and R_B are the ionic radii of A-site and B-site cations, respectively. R_O is the ionic radius of the anion.

Shannon's ionic radii are used to calculate t values [20]. The perovskite structures are stable when the t values are in the range of 0.75–1.00 [3]. The value of t was found to be 0.9897, which indicates the stablity of the perovskite structure.

Fig. 1 a shows the XRD pattern of the BNBT6: 4Eu sample. Enlarged portions of the XRD patterns in the 2θ ranges of 39–42^0 and 45–48^0 are shown in Fig. 1b and c, respectively. Eu^{3+} has diffused into the lattice to form a pure perovskite structure with rhombohedral symmetry. The characteristic (003) and (021) peak splitting between 39–42^0 shows the rhombohedral symmetry of BNT and the (002) and (200) peak splitting between 45–48^0 shows the tetragonal symmetry of BT [6]. This confirms the coexistence of the rhombohedral and tetragonal phases in the BNBT6: 4Eu system, which is consistent with the nature of the sample as a composition within the MPB [16].

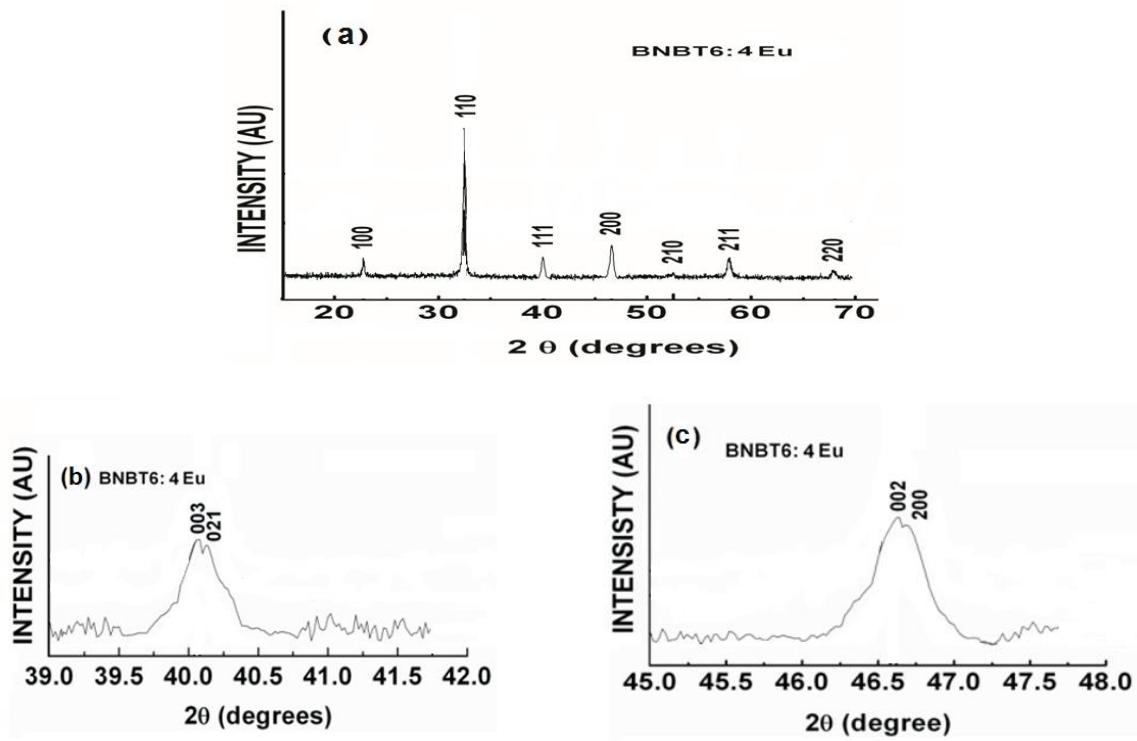

Figure1. *XRD patterns of BNBT6: 4Eu for 2θ in the range of (a) 10-80^0, (b) 39-42^0, and (c) 45-48^0*

The maximum intensity peak in BNBT6: 4Eu is observed at 2θ=32.49^0. The lattice parameters (a) and (α) are 3.878Å and 88.99 degree, respectively and the unit cell volume is 58.31Å^3. The experimental, theoretical and relative density of the BNBT6: 4Eu sample are 6.02 g/cm^3, 5.97 g/cm^3, and 99.11%, respectively. The SEM micrograph of BNBT6: 4Eu is shown in Fig. 2. Uniformly distributed rectangular grains were obtained. The average grain size, calculated by the mean linear intercept method, is 1.137 μm. Smaller average grain sizes imply Eu_2O_3 acts as grain growth inhibitor. Some SEM instruments have the very valuable additional feature of providing an elemental analysis of sample composition through Energy Dispersive X-ray Scanning (EDS/EDAX). Though EDS is not a surface science, it is used in conjunction with SEM for chemical microanalysis purpose. Only the elements present in the initial compounds were confirmed from the EDS spectra, in a fairly homogenous distribution throughout the grains, as shown in Fig. 3 [22].

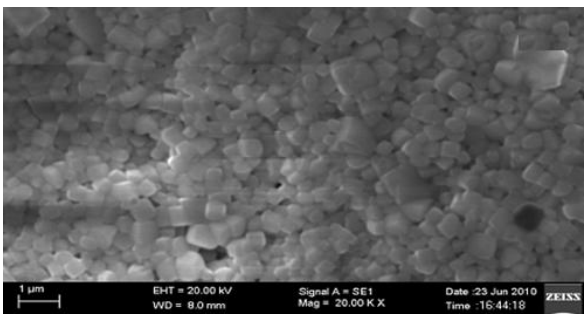

Figure2. *SEM micrographs of BNBT6: 4Eu*

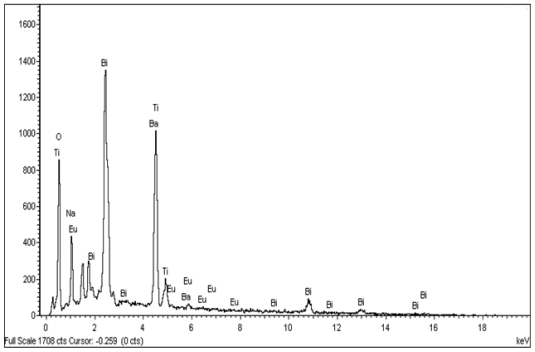

Figure3. *Energy Dispersive Spectra of BNBT6: 4Eu*

3.2. Piezoelectric Properties

The piezoelectric charge constant (d) is an important parameter of the suitability of a piezoelectric material for strain dependent applications such as actuators, since the strain induced by an applied electric field if the product of the value of d and E. The electromechanical coupling factor, k, indicates the effectiveness with which a piezoelectric material converts electrical energy in to mechanical energy or vice versa. For efficient energy conversion, a high k value is generally desirable. The efficiency of a typical piezoelectric ceramic at low frequencies lies in the range of 30-40%. The planar coupling factor, k_P, for a thin disc shaped piezoelectric ceramic indicates a radial coupling, that is, the coupling between an electric field in direction 3 (poling direction of the ceramic) and mechanical effects that produce radial vibration relative to the direction of polarization (direction 1 and 2). The mechanical quality factor, Q_M, is a dimensionless quantity given by the ratio of reactance to resistance. It indicates the sharpness of mechanical vibration in the resonant frequency

To enhance the values of piezoelectric property, we have added Eu_2O_3 into the lead-free BNT–BT solid solution and obtained d_{33}, k_p, and Q_M values of 158pC/N, 28%, and 100, respectively, at room temperature for BNBT6:4Eu sample. These relatively enhanced piezoelectric properties are assumed to be due to easier domain movement, since the strain caused by domain reorientation will be relaxed because of Na^+-site vacancies [6]. Eu^{3+} may enter into the Na^+-site and vacancies will be created to maintain charge neutrality arising from the difference between Eu^{3+} and Na^+. Also, lattice distortion might result when Eu^{3+} partially replaces Bi^{3+}, leading to easier domain reorientation during poling, which in turn enhances the piezoelectric properties.

In thickness mode, the piezoelectric d coefficient is defined as: $d_{33} = S/V = \Delta t/V \Rightarrow \Delta t = d_{33}V$. The change in thickness of the ceramic sample is dependent on the applied voltage and d_{33} but it is independent of the thickness (t) of the sample. The change in thickness (Δt) of the BNBT6:4Eu sample for an applied voltage of 100V is 15.8. Infinitesimally small Δt implies the BNBT6:4Eu sample could be useful in devices that regulate very small mechanical displacements. The amount of thickness change could be controlled by changing the applied voltage.

4. DIELECTRIC STUDY

One of the important electrical properties of dielectric materials is relative permittivity (ε_r), generally referred to as dielectric constant, which is strongly dependent on the frequency of the external AC electric field. It is defined as the ratio of the charge stored on a parallel-plate-capacitor filled with a dielectric material at a given voltage to the charge stored on identical parallel-plate-capacitor separated by a vacuum. In a real capacitor filled with a dielectric material between the conducting plates (electrodes) and connected to an AC electric field, there is a phase shift of δ, where the current leads the voltage by 90–δ degrees. The phase shift, δ is commonly called the loss angle, and the dielectric loss is defined as the tangent of the loss angle (tan δ).

Fig.4 shows the dependence of real part of dielectric constant (ε') on temperature, measured at selected frequencies in the range of 500 Hz to 10 kHz for the BNBT6: 4Eu sample. The dielectric constant curves exhibit two abnormal peaks attributed to phase transitions. The shoulder type peak at lower temperature (100 –200^{0}C) is called depolarization temperature (T_d) and corresponds to a transition from ferroelectric to "antiferroelectric" phase. The broad peak near the maximum temperature (T_m) corresponds to a transition from "antiferroelectric" to paraelectric phase. The maximum dielectric constant (ε'_{max}) was obtained at T_m. The dielectric constant increases gradually with increasing temperature up to T_m due to interfacial polarization dominating the dipolar polarization. The subsequent decrease in the dielectric constant above T_m is due to the phase change. The broad dielectric peaks at T_m suggests a diffuse phase transition (DPT) [23, 24].

Smolenski, *et al.*, was the first to observe such ferroelectric relaxor behavior in Ba (Ti, Sn) O_3 and Pb ($Mg_{1/3}Nb_{2/3}$) O_3 and called it *a behavior of the ferroelectric with diffuse phase transition*. Over the years, several theories have been suggested for the possible cause of the DPT behavior, namely: compositional fluctuations at the cation site, order-disorder transitions, microdomain to macrodomain switching, the presence of nanometer-scale polar regions in relaxors analogous to superparamagnets, the correlation between polar clusters in the dipolar-glass model, and the presence of domain states induced by quenched random fields. It has been reported that the ferroelectric relaxor behavior of a system is closely related to the appearance of the micropolar clusters in that system [25]. A continuous change from ferroelectric to relaxor behavior is unique feature of lead-free solid solutions [26].

The values of ε'_{RT} and ε'_{max}, at 1 kHz in the BNBT6: 4Eu sample are 1229 and 3322, respectively. In general, Eu_2O_3 substitution lowers the dielectric properties. The values of T_d and T_m in the BNBT6 : 4Eu sample at 1 kHz are 180^0C and 325^0C, respectively. The plausible reason for these low values of T_d and T_m in the BNBT6 : 4Eu sample could be suggested as follows. It is known that Bi^{3+}, Na^+, and Ba^{2+} are randomly distributed in the 12-fold coordination sites of the BNBT6 material and there is no long-range order of these cations in the A-sites of the sample. The principle of crystal chemistry dictates that a substituted ion preferably goes into the lattice by substituting the isovalent ion which has a similar radius [24]. The ionic radii of Ba^{2+}, Bi^{3+}, Na^+, Ti^{4+} and Eu^{3+} are 1.35 Å, 1.03 Å, 1.02 Å, 0.605 Å, 0.947 Å, respectively. Thus, in the BNBT6 sample, it is difficult for Eu^{3+} to enter into the B-site of Ti^{4+} because it is too big to substitute Ti^{4+} which has smaller radius than Eu^{3+}. Therefore, Eu^{3+} will most likely substitute Bi^{3+} at the A-site. It can be concluded that A-site substitution of Eu^{3+} in the BNBT6 system enhances the compositional inhomogeneity and reduces both T_d and T_m.

Another possible reason for the decrease in the value of T_d due to Eu_2O_3 content may be from the view point of the coupling reaction between A-site cation and BO_6 octahedron on the stability of ferroelectric domain walls. According to the theory of dielectric response of relaxor ferroelectrics discovered by Thomas, the stability of ferroelectric domain decreases when the coupling reaction between A-site cation and BO_6 octahedron decreases. It is known that the volatility of Bi^{3+} during high temperature sintering creates A-site vacancy which impairs the coupling reaction between A-site cations and the BO_6 (i.e., TiO_6) octahedron. Consequently, T_d (and the stability of ferroelectric domain) will be reduced [27].

An up turning of dielectric curve at much higher temperatures (> 470 ^{0}C) and lower frequencies (≤ 1 kHz) was observed in the BNBT6 : 4Eu sample. Most researchers agree that the peaks are not related to another phase transition. But, it seems that there is difference of opinion on the cause for the occurrence of the dielectric upturning.

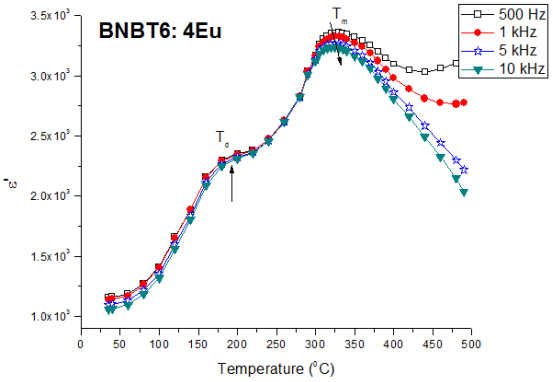

Figure4. *Real part of dielectric constant versus temperature at selected frequencies in BNBT6 : 4Eu*

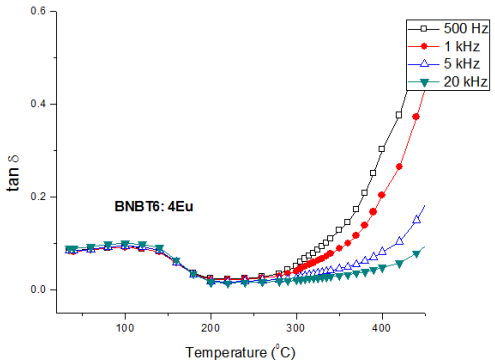

Figure5. *Dependence of tan δ on Temperature at selected frequencies in BNBT6 : 4Eu*

Fig. 5 shows the dependence of dielectric loss tangent (tan δ) on temperature, in the frequency range of 500 Hz–20 kHz for the BNBT6: 4Eu sample. The value of tan δ increases with frequency when the temperature is increased from RT to around 100–200 ^{0}C, which is attributed to sharp increase in the density and the movement of ferroelectric domain wall [2]. Dielectric loss tangent peak results due to enhancement of domain wall movement as a result of the phase transition from the ferroelectric to anti-ferroelectric phase near T_d, [17]. The loss peak reaches a maximum value at the depolarization temperature T_d, before it decreases drastically with increasing temperature above T_d for all the studied frequencies. The possible reasons are high conductivity of the samples at elevated temperatures, decreasing domain wall density and less distortion in the crystalline structure [6]. When the temperature is further increased above T_m, significant increase of tan δ occurred for lower frequencies while the value remained very low at higher frequencies (not indicated in the figure) [23]. The values of tan δ at RT and at T_m at1 kHz in the BNBT6: 4Eu are 0.070 and 0.062, respectively. The room temperature tan δ values were found to be very low in the sample.

The modified Curie–Weiss law is used to explain the diffuse phase transition and relaxor behavior in perovskite type relaxor ferroelectrics given by $1/\varepsilon' = (1/\varepsilon'_{max})[1 + (T - T_m)^{\gamma}/C]$ where, ε'_{max} is maximum permittivity at T_m, ε' is the permittivity, T is temperature above T_m (in the paraelectric region), C is a constant and γ is the diffuseness parameter representing the degree of dielectric relaxation ($1 \leq \gamma \leq 2$). For a normal ferroelectric with normal Curie–Weiss behavior, γ = 1. For a completely disordered ferroelectric, γ = 2. When $1 < \gamma < 2$, the material is called relaxor ferroelectric. Fig. 6 shows ln $[(\varepsilon'_{max}/\varepsilon') - 1]$ versus ln $(T - T_m)$ for the BNBT6 : 4Eu sample at 1 kHz. By linear fitting the experimental data using the modified Curie–Weiss law, it was found γ = 1.88, which indicates the diffuse nature of phase transition in the sample.

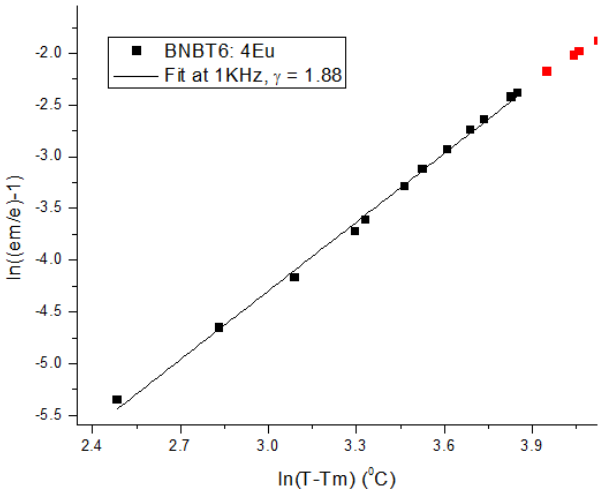

Figure6. *Dependence of ln $[(\varepsilon'_{max}/\varepsilon') - 1]$ on ln$(T - T_m)$ in BNBT6 : 4Eu*

Fig. 7 and 8 show the real part (ε') and imaginary part (ε") of the dielectric constant as a function of frequency, at different studied temperatures on log–log scales. The advantage of the double – logarithmic representation over the semi – logarithmic representation is that, the power law dependence is immediately recognizable in the double – logarithmic plot than the semi – logarithmic plot. Both ε' and ε" were found to be decreasing with increase in frequency in the BNBT6 : 4Eu sample with obvious dispersion in the low frequency region.

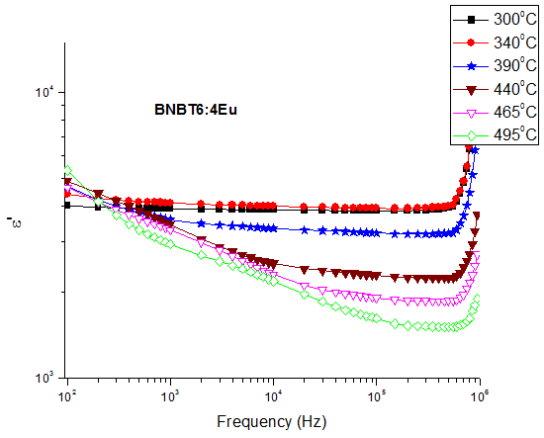

Figure7. *Frequency dependence of the real part (ε') of the Complex dielectric constant at different temperatures in BNBT6 : 4Eu*

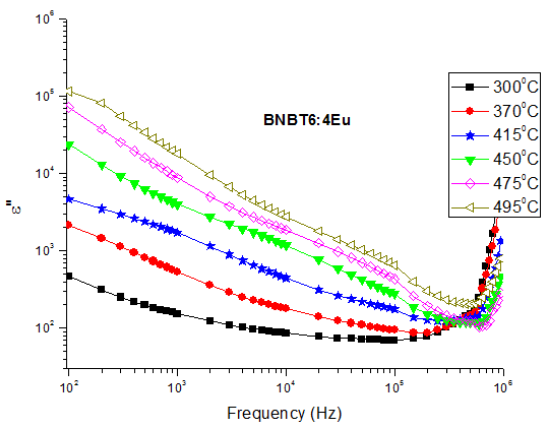

Figure8. *Frequency dependence of the imaginary part (ε") of the Complex dielectric constant at different temperatures in BNBT6 : 4Eu*

The space charge polarization, i.e., the migration and accumulation of electric charge carriers at the boundaries of homogenous phases in the external electric field as well as charge injection at the interface between the dielectric and the electrode are believed to be the cause for high value of ε' at

lower frequencies. The observed higher value of ε" at lower frequency is attributed to free-charge motion with in the material which is connected with the ac conductivity relaxation

5. IMPEDANCE SPECTROSCOPY

Impedance spectroscopy is a powerful method of characterizing many of the electrical properties of materials and their interfaces with electronically conducting electrodes [28]. The complex impedance (Z^*) is given by: $Z^* = Z' - jZ'' = R_s - 1/j\omega C_s$, where Z' and Z'' are the real and imaginary parts of impedance, respectively. R_s is series resistance, C_s is series capacitance, ω ($2\pi f$) is angular frequency.

Figure 9 shows real part of impedance (Z') versus frequency (100 Hz – 1 MHz) at different temperatures (430^0C – 490^0C) in the BNBT6 : 4Eu sample. Such data range usually allows the contributions of bulk (grain) lattice, grain boundary and electrode contributions to the impedance to be extracted. Z' has been strongly influenced by frequency as well as temperature. The value of Z' at 1 kHz has decreased from 126 kΩ to 17.6 kΩ as the temperature increased from 400^0C to 495^0C. In addition, high dispersion of Z' at lower frequency was observed.

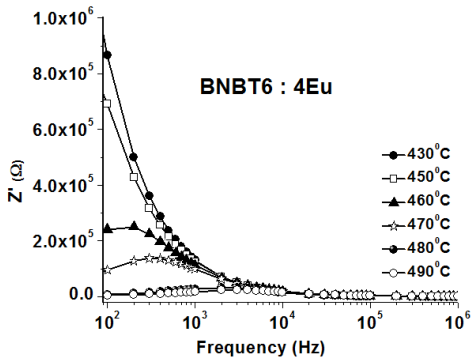

Figure9. *Real part of Impedance (Z') versus frequency at different temperatures in BNBT6 : 4Eu*

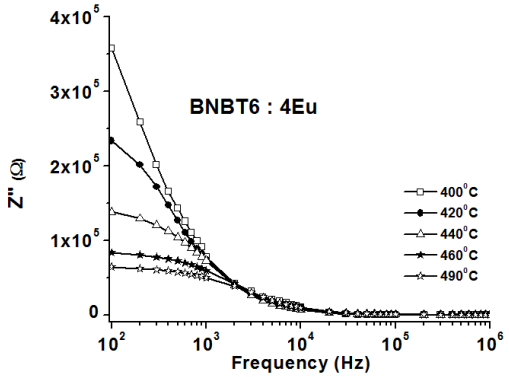

Figure10. *Dependence of imaginary part of impedance (Z") on frequency at different temperatures in BNBT6 : 4Eu*

The magnitude of Z' has higher values at lower frequencies and shows a monotonous decrease with increase in frequency for all the temperatures up to a certain frequency (~10 kHz). The decrease in Z' with increase in frequency and temperature indicates an increase in AC conductivity [28]. The Z' values merge above 10 kHz for all temperatures and become frequency independent which might be due to the release of space charge [28, 29] as a result of decrease in the barrier properties of the materials. The decrease of Z' with increasing temperature indicates the negative temperature coefficient of resistance (NTCR) type behavior in the studied sample similar to that of a semiconductor, reduction of grain and grain – boundaries resistances and increase in AC conductivity. Higher values of Z' at lower frequencies and temperatures implies larger effect of polarization. The temperatures where the change occurs vary with frequency, because the resistive grain boundaries become conductive at these temperatures, which indicate the grain boundaries are not relaxing even at very high frequencies and higher temperatures

The variation of the imaginary part of impedance (Z") with frequency at different temperatures (400^0C-490^0C) in the studied material is shown in Fig. 10. The advantage of Z" versus frequency representation is that the relaxation frequency could be evaluated to investigate the presence of space charge polarization. In the BNBT6 : 4Eu sample at 1 kHz, when the temperature was increased from 400^0C to 495^0C, the value of Z" decreased from 77.5 kΩ to 50 kΩ. More over, at lower temperatures (<440^0C) Z" has decreased monotonously with increase in frequency which is suggestive of the absence of any relaxation. The relaxation species in the material are immobile species/electrons and orientation effects might have been involved in all the samples [30]. The studied sample exhibited Z" plot which continuously decreased with increase in frequency up to 10 kHz for all temperatures. The Z" curves merged with one another at higher frequencies (above 10 kHz) irrespective of temperature. The Z" peaks shifted towards higher frequency side and the peak height decreased with increasing temperature.

The normalized imaginary part (Z''/Z''_{max}) of impedance as a function of frequency in the BNBT6 : 4Eu sample at different temperatures is shown in Fig. 11. The Z''/Z''_{max} parameters exhibited slightly

asymmetric broadening at high temperatures which indicate the triggering of another temperature-dependent relaxation process [30]. The Z''/Z''_{max} peak values shifted to higher frequency side with increase in frequency.

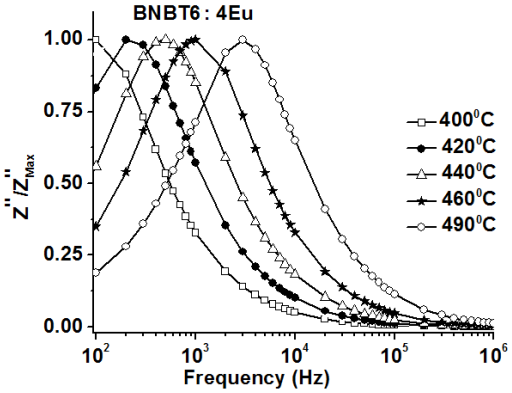

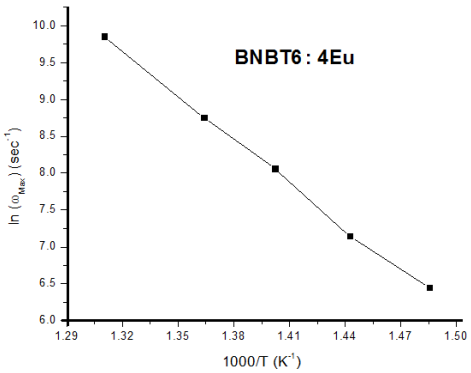

Figure11. *Normalized imaginary part of impedance (Z''/Z''_{max}) versus frequency at different temperatures in BNBT6 : 4Eu*

Figure12. *Dependence of Relaxation Frequency on Temperature in BNBT6 : 4E*

In a relaxation system, the most probable angular frequency ($\omega_m = 2\pi f_m$) could be determined from the position of the loss peak in the Z'' versus relaxation frequency plots using the following relation

$$\omega_m \tau_m = 1$$

Where τ_m is the peak relaxation time and ω_m is maximum angular frequency

When the temperature is increased, ω_m has been increased which is indicative of the negative temperature coefficient of resistance (NTCR) behavior similar to a semiconductor material, believed to be due to the loss of oxygen ions during high temperature sintering process. Fig. 12 shows the activation energy E_τ calculated from log ω_m versus 1000/T. The values of E_τ obtained from the Arrhenius plots for BNBT6: 4Eu is 0.57eV. Low value of relaxation activation energy suggests the conduction is ionic in nature in the studied sample. Also, small value of activation energy imply higher mobility of oxygen vacancies which are one of the mobile charge carriers.

Variation of Z'' and Z' as a function of frequency in the BNBT6 : 4Eu sample at different temperatures is shown in Fig. 13. When the frequency is increased, Z' value was decreased while Z'' was increased and reached to a peak value, Z''_{max}. With further increase of frequency above Z'' peak frequency, both Z' and Z'' values have decreased. At higher frequencies (above 10 kHz), both Z' and Z'' have significantly decreased and subsequently merged with the horizontal axis. The frequency of intersection for Z' and Z'' is to the right side of the peak frequency of Z''_{max}. As the temperature increases, the intersection frequency of Z' and Z'' shifts towards higher frequency side. This indicates that there exists a relaxation phenomenon [29].

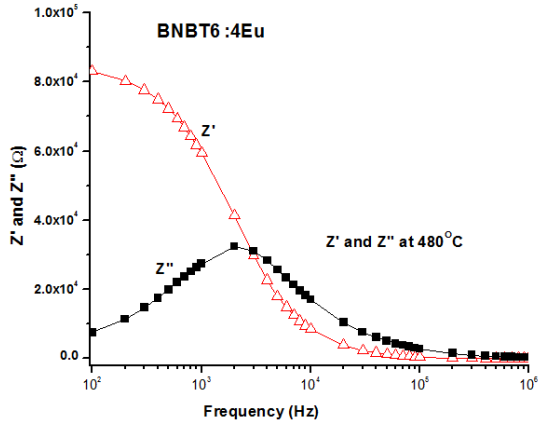

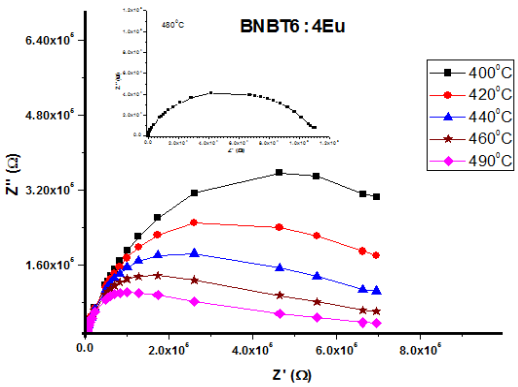

Figure13. *Real and Imaginary parts of impedance (Z' and Z'') versus frequency in BNBT6 : 4Eu*

Figure14. *Imaginary parts of impedance (Z'') versus Real parts of impedance (Z') in BNBT6 : 4Eu*

Imaginary part of impedance (Z") versus real part of impedance (Z') is shown in Fig. 14. The complex impedance spectra of the electrode-ceramic-electrode capacitor can be modeled as the sum of parallel RC-circuit combinations. The effect of temperature on the response becomes more prominent at higher temperature which is characterized by the number of semicircular arcs.

In the BNBT6 : 4Eu sample, the centers of the semicircles lie below the Z' axis indicating non – Debye type relaxation mechanism in the material [2]. Furthermore, when the temperature is increased, the peak maxima of the plots have decreased and the frequencies for the maxima shifted to higher frequency values indicating increase in conductivity of the sample [20]. The parallel RC-circuit model was used to calculate the fitting parameters: R_g, C_g, R_{gb}, C_{gb}, τ_g, and τ_{gb}, given in Table 2. In the BNBT6 : 4Eu sample, the values of R_g decreased from 250 kΩ to 40 kΩ and R_{gb} decreased from 475 kΩ to 68 kΩ when the temperature was increased from 430 to 490^0C. A decrease in the value of R_g with increase in temperature indicates an increase in conductivity, while a decrease in R_{gb} with increase in temperature suggests the lowering of the barrier to the mobility of charge carriers and increasing electrical conduction at higher temperatures [29]. Thus, temperature and microstructure influence the electrical properties in the BNBT6 : 4Eu sample.

The grain boundary capacitance (C_{gb}) and the grain boundary relaxation time (τ_{gb}) are calculated from $\omega_{gb,max} = 1/(R_{gb}C_{gb}) = 1/\tau_{gb}$, respectively. The values of C_g and C_{gb} decreased from 2.38 nF to 0.985 nF and from 7.31 nF to 2.34 nF, respectively while τ_g and τ_{gb} values decreased from 594 μs to 39.4 μs and from 3470 μs to 159 μs, respectively, when temperature was increased from 430^0C to 490^0C. More over, the trend in the BNBT6 : 4Eu sample is such that Z' and Z" values are effectively larger at low temperatures and low frequencies, predominantly due to the effect of polarization.

At higher temperatures one can see depressed semicircles which could be resolved into two semicircular arcs. The appearance of the second semicircular arc indicates the beginning of the grain boundary effect within the composition with definite contributions from both grain and grain boundary effects. The radii of the semicircular arcs have been found to shift toward the origin on the Z' axis which indicate the decrease in grain resistance (R_g) and grain boundary resistance (R_{gb}) with increase in temperature, which is consistent with the above data.

Table2. *Grain and grain boundary fitting parameters at selected temperatures in BNBT6:4Eu*

Temp (^{0}C)	R_g (KΩ)	C_g (nF)	τ_g (μsec)	R_{gb} (KΩ)	C_{gb} (nF)	τ_{gb} (μsec)
430	250	2.38	594	475	7.31	3470
460	140	1.25	175	252	2.87	722
490	40	0.985	39.4	68	2.34	159

Fig. 15 and 16 show Arrhenius plots of the grain and grain boundary resistance and capacitance, respectively in the BNBT6 : 4Eu sample. The grain conduction energy (E_g), grain boundary conduction energy (E_{gb}), grain relaxation energy (ε_g) and grain boundary relaxation energy (ε_{gb}) values of the sample at different temperatures (400^0C-490^0C) are given in table 3. The grain conduction energy is found to be lower than the grain boundary conduction energy ($E_g < E_{gb}$) indicating higher grain boundary resistive behavior than that of the grains. Since, the conduction takes place through the low resistance path, by viewing calculated values of the grain and grain boundary resistances, it can be seen the conduction path is predominantly through the grains [31]. Thus, one can conclude that the grain boundaries resistances are the dominant factors for the overall electrical behavior of the material.

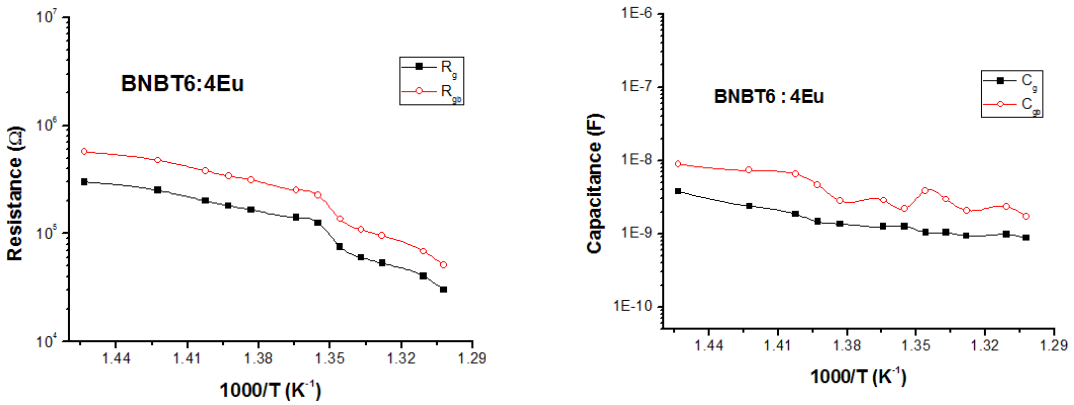

Figure15. *Dependence of grain and grain boundary resistance on temperature for BNBT6 : 4Eu*

Figure16. *Dependence of grain and grain boundary capacitance on temperature for BNBT6 : 4Eu*

Table3. *Activation energy values for E_g, E_{gb}, ε_g and ε_{gb} in BNBT6 : 4Eu sample*

Temperature (^{0}C)	E_g (ev)	E_{gb} (eV)	ε_g (eV)	ε_{gb} (eV)
440-490	0.59	0.65	0.59	0.58

6. CONCLUSION

Polycrystalline $(Bi_{0.90}Eu_{0.04}Na_{0.94})_{0.5}Ba_{0.06}TiO_3$ – BNBT6 : 4Eu ceramic composition was prepared by the conventional high temperature solid-state reaction method. A homogeneous and single phase perovskite-type structure was confirmed by XRD analysis.

- Highly dense ceramic sample with relative density of 99.11% was achieved.
- The obtained values of tolerance factor, t = 0.9897 indicates the studied sample has stable perovskite structure.
- Lattice parameter values (a) and (α) are 3.878Å and 88.99 degree, respectively.
- Uniformly distributed small rectangular grains have been observed from SEM micrograph.
- EDS spectrum shows only the elements constituting the starting powder compounds, that is, Bi, Na, Ba, Ti, O, Eu were found in the BNBT6 : 4Eu sample.
- In the studied sample, d_{33}= 158pC/N, k_P = 28%, and Q_M = 100 were obtained.
- ΔT = 15.8nm to an applied voltage of 100 V was achieved. Therefore, the BNBT6 : 4Eu composition is a very good candidate for device applications which require very small and precise displacement, such as in actuators.
- The BNBT6 : 4Eu sample was found to exhibit relaxor ferroelectric behavior with diffuse phase transition.
- The value of the diffuseness constant, γ = 1.88.
- The value of room temperature dielectric constant, ε_{RT}=1229 was achieved in the sample.
- Low frequency dielectric dispersion (LFDD) has been observed at lower frequencies which might be due to electrode polarization.
- The value of dielectric loss tangent (tan δ) were found to be very low, of the order 0f 10^{-2} revealing the studied sample is a low loss compositions.
- Dielectric loss dispersion around 100-200^{0}C has been observed in the studied sample.
- Negative temperature coefficient of resistance (NTCR) behavior was exhibited in the sample.
- In the BNBT6: 4Eu sample, the value of activation energy, E_τ = 0.57 5eV.
- Maximum value of R_g = 250 kΩ and R_{gb} = 475 kΩ were achieved in the BNBT6 : 4Eu sample.
- The centeres of the semicircular arcs in the Cole-Cole plots (Z″ versus Z′ plots) were found to lie below the horizontal axis (Z′-axis), indicative of non-Debye type process.
- Similar type of behavior on C_g, C_{gb}, τ_g and τ_{gb} has been observed.

REFERENCES

[1] B. Jaffe, W.R. Cook and H. Jaffe, Academic, New York, 1971.

[2] P. Fu, Z. Xu, R. Chu, W. Li, Q. Xie, Y. Zhang, Q. Chen, J. Alloys Compd. (2010), doi:10.1016/j.jallcom.2010.08.117.

[3] S. R. McLaughlin, Ph. D. dissertation, Queen's University, Kingston, Ontario, Canada, 2008.

[4] Q. Zheng, C. Xu, D. Lin, D. Gao and K.W. Kwok, J. Appl. Phys. D 41 (2008) 125411.

[5] G.A. Smolenskii,V.A. Isupov, A.I. Agranovskaya and N.N. Krainik, Fizika, Sov. Phys. Solid State 2 (11) (1961) 2651–2654.

[6] X.X. Wang, H.L.W. Chan, C.L. Choy, Appl. Phys. A: Mater Sci. Process 80 (2005) 333–336.

[7] C.-S. Tu, I.G. Siny and V.H. Schmidt, Phys. Rev. B: Condens. Matter Mater. Phys., Vol. 49 (17) (1994) I.

[8] J. Suchanicz, Ferroelectrics 200 (1977) 319–325.

[9] J. Suchanicz, Ferroelectrics, 209 (1998) 561–568.

[10] Y. Lin, S. Zhao, N. Cai, J. Wu, X. Zhou, C.W. Nan, Mater. Sci. Eng., B 99 (2003) 449–452.

[11] M. Raghavender, G.S. Kumar and G. Prasad, Indian J. Phys. 72 (6) (2009) 999–1009.

[12] A. Watcharapasorn, Ceram. Int. 34 (2008) 769–772.

[13] S. Mahboob, G. Prasad, G.S. Kumar, J. Mater Sci. 42 (2007) 10275–10283

[14] T. Takenaka, H. Nagata and Y. Hiruma, Jpn. J. Appl. Phys. 47, No. 5, (2008) 3787–3801.

[15] H.-D. Li, C.-D. FENG and W.-L. Yao, Mater. Lett. 58 (2004) 1194–1198.

[16] J. Shi, W. Yang, J. Alloys Compd. 472 (2009) 267–270.

[17] C. Zhou, X. Liu, W. Li and C. Yuan, Mater. Res. Bull. 44 (2009) 724–727.

[18] A.R. West, Solid State Chemistry and its Applications, John Wiley & Sons, Singapore, 1998.

[19] Q. Xu, M. Chen, W. Chen, H.-X. Liu, B.-H. Kim, B.-K. Ahn, J. Alloys Compd. 463 (2008) 275–281.

[20] http://abulafia.mt.ic.ac.uk/shannon/ptable.php. Accessed on April 4, 2010.

[21] A.I., Agranovskaya, IZV. Akad. Nauk SSSR, Ser. Fiz. 24 (1960) 1275.

[22] M. Adamczyk, Z. Ujma, M. Paweczyk, J. Mater. Sci. 41 (2006) 5317–5322.

[23] W. Ge, H. Liu, X. Zhao, B. Fang, X. Li, F. Wang, D. Zhou, P. Yu, X. Pan, D. Lin and H. Luo, J. Appl. Phys. 41 (2008) 125403–125407.

[24] H.-D. Li, C.-D. Feng and P.-H. Xiang, Jpn. J. Appl. Phys. 1(2003).

[25] C. Ang, Z. Yu and Z. Jing, Phys. Rev. B: Condens. Matter Mater. Phys. 61 (2000) II

[26] R.G. Palmer, D.L. Stein, E. Abrahams, Phys. Rev. Lett. 53 (1984)

[27] J. Shi, W. Yang, J. Alloys Compd. 472 (2009) 267-270.

[28] A. Simon, J. Ravez and M. Maglione, J. Phys.: Condens. Matter 16 (2004) 963–970.

[29] E. Barasoukov, J.R. Macdonald, Impedance Spectroscopy, Theory, Experiment, and Applications, Second ed., John Wiley & Sons, New Jersey, 2005.

[30] S. Sen, P. Pramanik and R.N.P. Choudhary, Appl. Phys. A: Mater. Sci. Processss 82 (2006) 549.

[31] S. Mahajan, O.P. Thakur, D.K. Bhattacharaya and K. Sreenivas, J. Appl. Phys. 42 (2009) 065413.

[32] N. Hirose and A.R. West, J. Am. Ceram. Soc. 79 (1996) 1633.